State of Oregon
Department of Geology and Mineral Industries
910 State Office Building
Portland, Oregon 97201

OPEN-FILE REPORT O-86-18

HYDROTHERMAL PRECIPITATES FROM BASALTS ON THE GORDA RIDGE AND THE PRESIDENT JACKSON SEAMOUNTS

By Katherine J. Howard and Martin R. Fisk,
College of Oceanography, Oregon State University,
Corvallis, Oregon 97331

Final Report for Contract No. 63-630-8508

Submitted to:

Oregon Department of Geology and Mineral Industries

and the

Gorda Ridge Technical Task Force

Released December 1986

NOTICE

This report is based on results of a research program directed by the joint federal-state Gorda Ridge Technical Task Force, managed by the Oregon Department of Geology and Mineral Industries and funded by the Minerals Management Service, U.S. Department of the Interior, through Cooperative Agreement. Opinions expressed are those of the authors and do not constitute endorsement by the sponsoring agencies or the Task Force.

The Oregon Department of Geology and Mineral Industries is publishing this paper because the subject matter is consistent with the mission of the Department. To facilitate timely distribution of information, camera-ready copy submitted by the authors has not been edited by the staff of the Oregon Department of Geology and Mineral Industries.

CONTENTS

LIST OF TABLES

LIST OF FIGURES

ABSTRACT

Hot springs in the axial valleys of ocean ridges produce a large variety of precipitates where the water exits from the sea floor. The most spectacular of these are the 30 to 40 m high chimneys composed of massive sulphides that have recently been discovered on a number of ocean ridges including the Gorda Ridge and Juan de Fuca Ridge in the northeast Pacific Ocean. The chimneys are centers of outflow of hot water laden with particulate matter and also the centers for precipitation of a wide variety of minerals of economic importance. Although these chimneys are the most spectacular of hydrothermal deposits, because they are the centers of large volumes of flow, hot water also seeps from cracks throughout the wide area in the vicinity of axial valleys and seamounts. These lower volume seeps will also deposit minerals when the hot water comes in contact with sea water and, because these seeps cover a large area compared to the smokers, identification of minerals indicative of hydrothermal activity in these precipitates could point the way to active hot springs and associated massive sulfide deposits. Such deposits may also be economically important because of the wide range of elements that are dissolved in the hot water and their potentially large areal extent.

Precipitates were removed from rocks in the Oregon State University collection and from rocks dredged by the USGS during the cruise of the S.P. Lee in 1985. Analysis by x-ray diffraction and by atomic absorption shows these deposits to be primarily hydrothermal clays and iron-manganese oxides. Minor amounts of sulfides, and possibly sulfates, arsenides, or arsenates, may be present in some samples. Extensive dredging on the northern end of the Gorda Ridge showed that the whole area had hydrothermal deposits on the surfaces of the rocks. Also the President Jackson Seamounts have deposits that are chemically distinct from deposits on the ridge axis. The samples from the OSU collection are also primarily hydrothermal clays indicating a source near an active hydrothermal area on the Gorda Ridge.

INTRODUCTION

Hydrothermal deposits

Sea water that penetrates the oceanic crust on oceanic ridges is heated by reservoirs of magma and this hot sea water leaches metals from the basalts through which it flows. The principal chemical components derived from the basalts, in addition to those already found in sea water, are silica, potassium and calcium. Other elements enriched in the hot water expelled onto the seafloor are lithium, rubidium, beryllium, strontium, and certain metals of special interest such as manganese, iron, cobalt, copper, zinc, silver, cadmium, and lead (Von Damm, et al., 1985). These elements are deposited on the seafloor in the form of oxides, hydroxides, sulfates, sulfides or silicate minerals as the hot hydrothermal waters cool or oxidize upon mixing with ambient seawater (Humphries and Thompson, 1978).

The distribution of metalliferous sediments and Fe and Mn concentrations in seawater around ridge axis rise crests have been used as prospecting tools (Dymond, 1981, Bäcker et al., 1985, Roth and Dymond, 1986) and these same concepts may also be applied to hydrothermal precipitations on dredged basalts. Local topography, such as enclosed basins, may enhance the formation of massive sulfide deposits and this can be used along with chemical data to determine sites most likely to contain such deposits (Edmond et al., 1979). Leaching from basalts requires temperatures in excess of 150^{o}C for mobilization of heavy metals (Edmond et al., 1979) and even higher temperatures (300-400^{o}C) are predicted for efficient transfer of metals into solution under rock dominated conditions (Mottl, 1983). Because of the abrupt change of conditions as the water exits from the vents on the seafloor, different minerals can precipitate sequentially over short distances, producing colored bands on surfaces of basalt near the vent. An example of this type of mineral zoning is shown in Figure 1 for a basalt sample from the northen end of the Gorda Ridge. The mineralogy and composition of these deposits reflect the temperature and composition of the hydrothermal source fluids and may be indicators of proximity to hydrothermal vents and associated massive sulfide deposits at the surface or deep in the oceanic crust (Lafitte et al, 1985).

Color

The precipitates observed on Gorda Ridge basalts vary widely in color. Individual layers can be black, tan, red, yellow, orange, brown or white and many layers are mixtures of these colors. Hydrothermal deposits found in vesicles or voids in the basalt form distinct crystalline phases that are yellow or white in color. Mixtures of colors probably represent a mixture of minerals and the short distance between colored bands on a single rock surface suggests that each mineral band precipitates within a narrow temperature range as the hot water exits from a vent. Color zoning could also reflect secondary oxidation after the precipitates form. In some cases sequences of bands appear more than once on the same

rock surface. One example of this is in OSU sample W7605B-4-44 (Fig. 1) which has the sequence (from outside to inside) of black, yellow, tan repeated three times in the space of 10 cm. These sequences may reflect episodic changes in the vigor and thermochemistry of hydrothermal activity. The chemical composition and mineralogy of these mineral bands were determined in this study.

Mineralogy

Sulfide chimneys from hydrothermal areas of ocean ridges are described as having three zones surrounding the venting hot water. The inner zone is made up primarily of chalcopyrite, the intermediate zone is made up of chalcopyrite, pyrite, sphalerite, bornite and anhydrite, and the outer margin is primarily anhydrite, with lesser amounts of the same sulfides found in the other zones along with iron-manganese oxides (Hekinian et al., 1983). The sulfide mineral zonation is probably the result of decreasing temperature of precipitation as vent waters migrate outward through the chimney walls (Koski et al, 1984).

Minerals that have been identified in hydrothermal deposits are listed in Table 1. These minerals contain the majority of elements commonly found in seafloor hydrothermal deposits. These include iron, manganese, copper, zinc, nickel, cobalt, and sulfur. Sulfide deposits on land are also known for their high concentrations of other elements such as lead, silver, gold, and platinum group metals.

Rapid changes of pressure, temperature, pH, and oxidation state affecting hydrothermal solutions exiting from seafloor vents, coupled with the large variety of contained metals, results in the precipitation of small quantities of many different minerals. Stability of these minerals following changes in the conditions of precipitation is unknown. They may alter to new minerals, redissolve in sea water, or act as sites of nucleation for more minerals of the same type. Some minerals may have been modified by bacterial scavenging (eg by Mn-oxidizing bacteria) (Edmond et al., 1979).

For these reasons, mineralogical analysis of the hydrothermal deposits is quite difficult. The x-ray diffraction patterns that are produced for a single color band on a basalt often represent a mixture of several minerals with interfering peaks. Positive identification of a mineral is often difficult, requiring detailed matches of several peaks and stripping away of competing peaks from other minerals. For example, in samples containing albite as a major constituent, removal of these peaks from the analysis permitted identification of smaller quantities of hydrothermal clays and oxides.

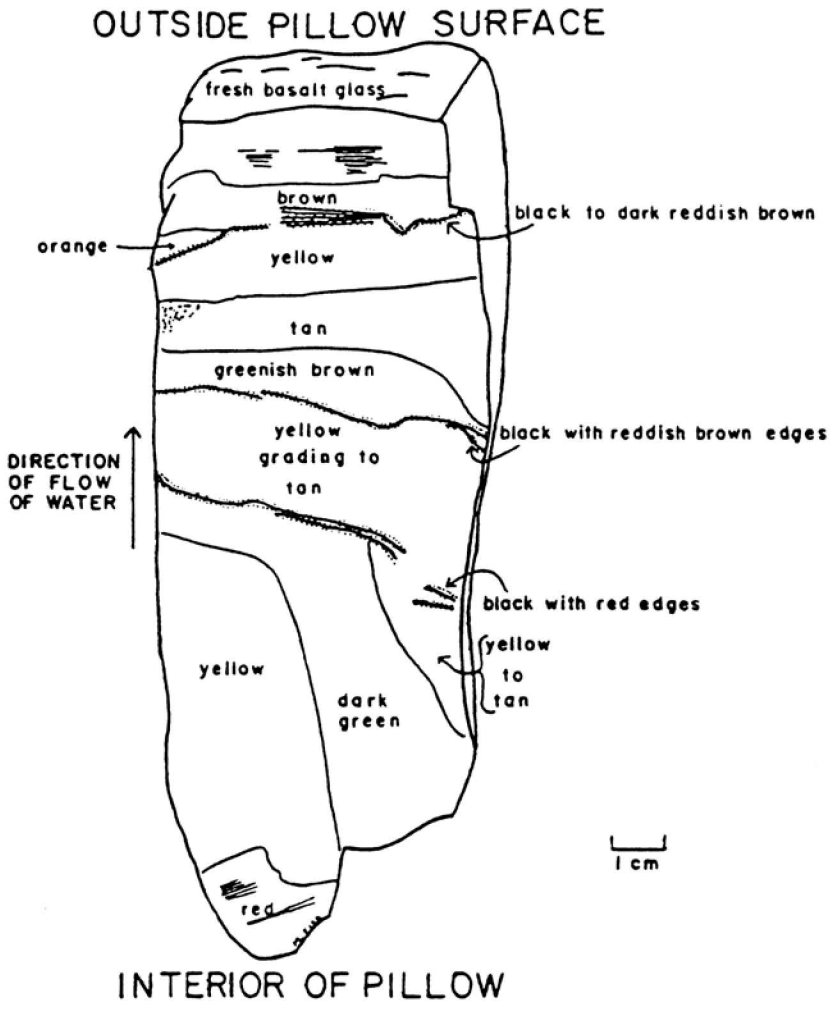

Figure 1: Drawing of a pillow fragment exhibiting distinct banding of mineral precipitates. Individual colors may represent minerals formed sequentially at specific temperatures as water flows through a fracture to the seafloor. In this particular example, (OSU sample W7605B-4-44) a pattern of black, yellow, tan (from outside to inside) is repeated three times within 10cm.

TABLE 1

Minerals commonly associated with hydrothermal deposits.

Oxides, hydroxides and oxyhydroxides	Silicates	Sulfides	Sulfates
Fe	smectite	Fe	barite
goethite	nontronite	pyrite	anhydrite
hematite	quartz	pyrrhotite	
Mn	opal	Cu-Fe	
birnessite	albite	bornite	
todorokite	zeolites	chalcopyrite	
δMnO_2	phillipsite	Zn	
	analcite	sphalerite	
	chlorite		
	clinochlore		

Additional minerals that may be present in small quantities.

Oxides, hydroxides and oxyhydroxides	Silicates	Sulfides	Sulfates
atacamite	smectite	Fe	gypsum
Fe	sepiolite	marcasite	jarosite
limonite	saponite	Cu-Fe	natro-
akaganieite	vermiculite	covellite	jarosite
lepidocrosite	celadonite	chalcopyrrhotite	alunite
maghemite-	serpentine	digenite	anglesite
magnetite	amesite	idaite	caminite
Mn	talc	chalcocite	Fe-sulfates
ranceite	Zeolites	cubanite	Zn-sulfates
natrobirnessite	stilbite	valleriite	
nsutite	heulandite	Zn	
manjiroite	clinoptilolite	wurtzite	
manganite	erionite	galena	
Al		tennantite	
boehmite		jordanite	
corundum*			

* tentatively identified by Haymon and Kastner (1981).

Other mineral species sometimes associated with hydrothermal activity that are likely to be present in small quantities are arsenides, and carbonates (eg. calcite, manganosiderite, magnesite).

(Clague et al., 1984, Haymon and Kastner, 1981, 1986a, 1986b, Koski et al., 1984, 1985, Hekinian and Fouquet, 1985, Oudin, 1983, Singer and Stoffers, 1981, Thompson et al., 1985, Whitney, 1983, Wirshing, 1981).

METHODS

Samples

The material analyzed in this study was obtained from the Oregon State University collection and from samples dredged from the Gorda Ridge and the President Jackson Seamounts during the USGS cruise L5-85-NC. Twenty-one samples from the OSU collection and twenty-nine samples from the USGS collection were analyzed by x-ray diffraction. In addition thirty of these samples were analyzed by atomic absorption. The locations of the sites from which our samples were collected are indicated in Figures 2a and b and Table 2.

Sampling

Material for analysis was removed from the exterior of the basalts and caution was taken to prevent the cross contamination of individual layers on a single rock. In some instances it was not possible to separate individual colored bands because of their small size relative to 1 mg of material needed for x-ray diffraction analysis.

Techniques

X-ray diffraction patterns were obtained using an automated SCINTAG x-ray diffractometer. The sample was mounted on a glass disk and rotated while the detector scanned continuously at 1 degree per minute over the 2θ range of interest. Background signals were removed from the spectrum and peaks selected by a standard computer routine. The peaks were compared to those in the inorganic mineral file of JCPDS, and minerals that matched three or more peaks were selected for further analysis.

Atomic absorption analyses were completed using standard techniques on a Perkin-Elmer 5000 atomic absorption spectrophotometer. The samples were analyzed for Si, Al, Ti, Ca, Mg, Na, K, Fe, Mn, V, Ba, Sr, Li, Rb, Cu, Ni, Zn, and Co. The precision of the analysis is about $\pm$ 2% for most elements but is $\pm$ 4% for silicon, iron and barium, based on the standard deviation of three analyses of a standard manganese nodule.

RESULTS

X-ray diffraction

Examples of diffraction patterns for three types of material collected from the thin hydrothermal deposits on basalts are shown in Figures 3, 4 and 5. In Figure 3, the four major peaks for todorokite, a manganese oxide, can be distinguished, although quartz makes up the dominant part of the sample. Figure 4 shows the major peaks for clinochlore, a clay mineral that forms at moderately high temperatures (probably > 150^{o}C) (Seyfried and Bischoff, 1979, Thompson, 1983). Unlabeled peaks in Figure 4 are associated with the

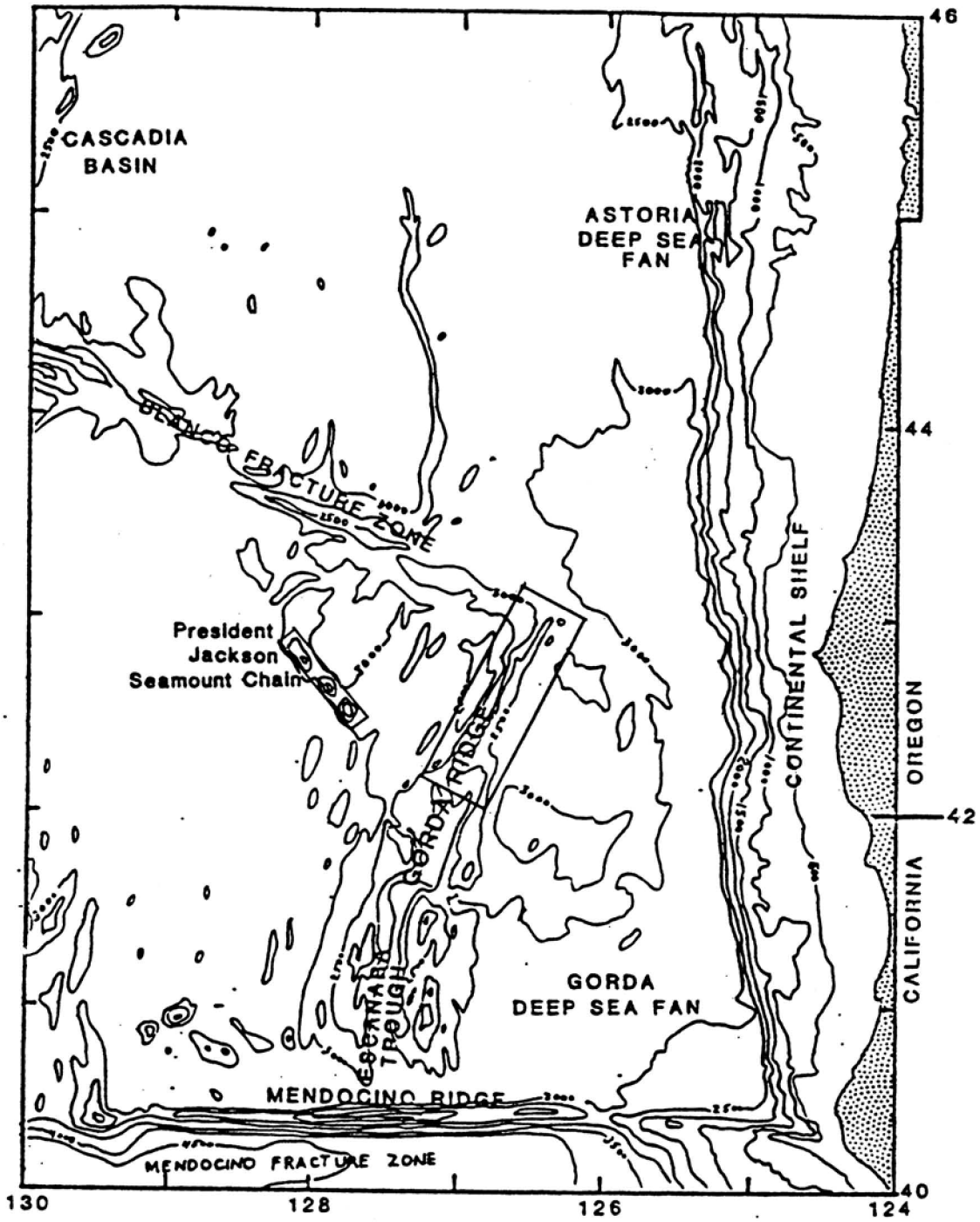

Figure 2a: Bathymetric map of the Gorda Ridge off the coast of Oregon and California after Wilde et al., 1978, 1979. Dredge sites from which samples were collected for this study are located in the boxed portions on the northern end of the ridge and President Jackson Seamounts. Contour interval is 500m.

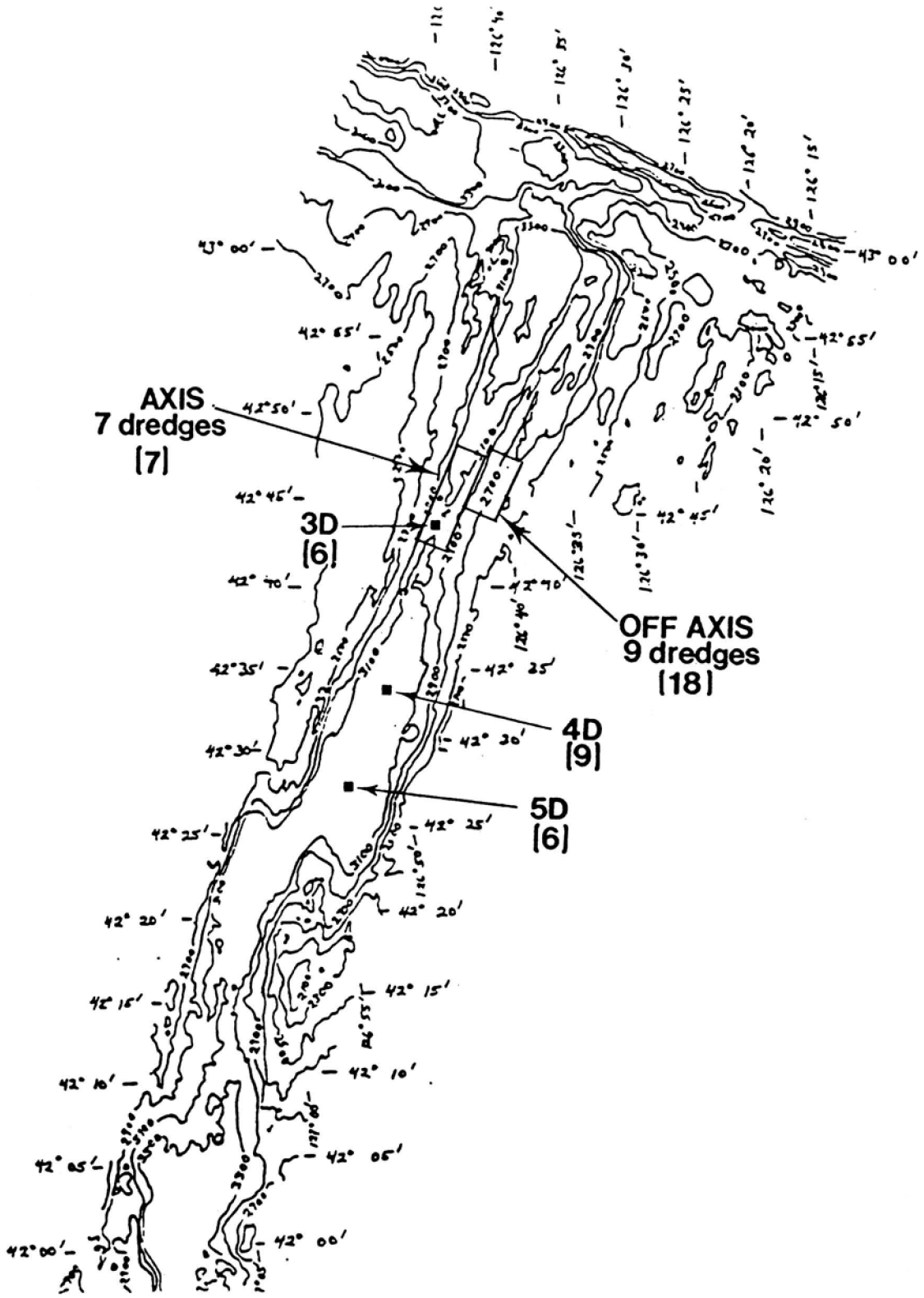

Figure 2b: Detailed bathymetry of the northern portion of the Gorda Ridge (from NOAA seabeam) with location of dredge sites from which material was collected for analysis. Areas labeled AXIS and OFF AXIS indicate locations of high density dredge sites from R/V S.P. Lee cruise L5-85-NC. The number of dredge sites within each delineated region is as indicated. Squares labeled 3D, 4D, and 5D indicate locations of dredge sites from OSU cruise W7605B. Numbers in ( ) indicate how many samples were analyzed from that region.

TABLE 2

Location and depth of dredge stations* from which samples were selected.

Gorda Ridge OSU Cruise W7605B

Dredge	Location	Depth
3D	42° 44'N, 126° 46'W	3000m
4D	42° 33'N, 126° 51'W	3666m
5D	42° 28'N, 126° 55'W	3690m

Gorda Ridge USGS Cruise L5-85-NC

Dredge	Location	Depth
On axis:		
38D	42° 47.16'N, 126° 43.24'W	3045m
39D	42° 45.96'N, 126° 44.08'W	3031m
40D	42° 45.57'N, 126° 44.65'W	3026m
42D	42° 47.92'N, 126° 42.09'W	3141m
43D	42° 45.00'N, 126° 45.00'W	2994m
44D	42° 45.54'N, 126° 44.83'W	2994m
45D	42° 42.29'N, 126° 45.42'W	3520m
Off axis:		
2D	42° 45.70'N, 126° 42.08'W	2745m
3D	42° 45.23'N, 126° 40.65'W	2682m
4D	42° 45.55'N, 126° 41.29'W	2675m
6D	42° 45.30'N, 126° 42.13'W	2690m
7D	42° 45.54'N, 126° 42.20'W	2594m
8D	42° 45.66'N, 126° 42.37'W	2734m
10D	42° 43.38'N, 126° 42.59'W	2719m
11D	42° 44.93'N, 126° 43.25'W	2720m
13D	42° 45.55'N, 126° 43.97'W	3075m
President Jackson Seamounts:		
29D	42° 50.35'N, 128° 12.21'W	2150m
32D	42° 44.32'N, 128° 05.69'W	1626m
33D	42° 44.04'N, 128° 06.40'W	1563m
34D	42° 32.00'N, 127° 47.00'W	2482m
35D	42° 24.75'N, 127° 41.01'W	2274m
36D	42° 25.66'N, 127° 40.76'W	1978m

* Locations and depths are from start of dredge.

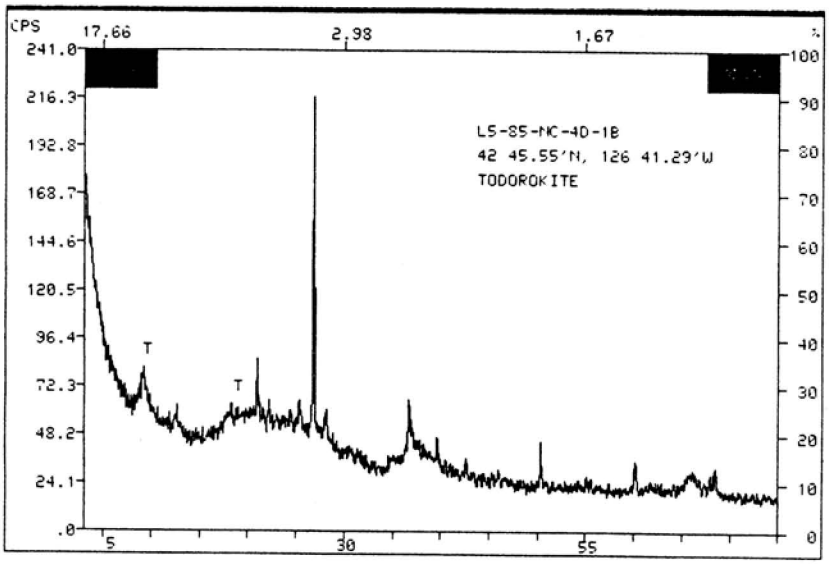

Figure 3: X-ray diffraction spectrum of sample L5-85-NC-4D-1B showing two major peaks for todorokite, Mn oxide (labeled T). Other major peaks are from the SiO_2 internal standard.

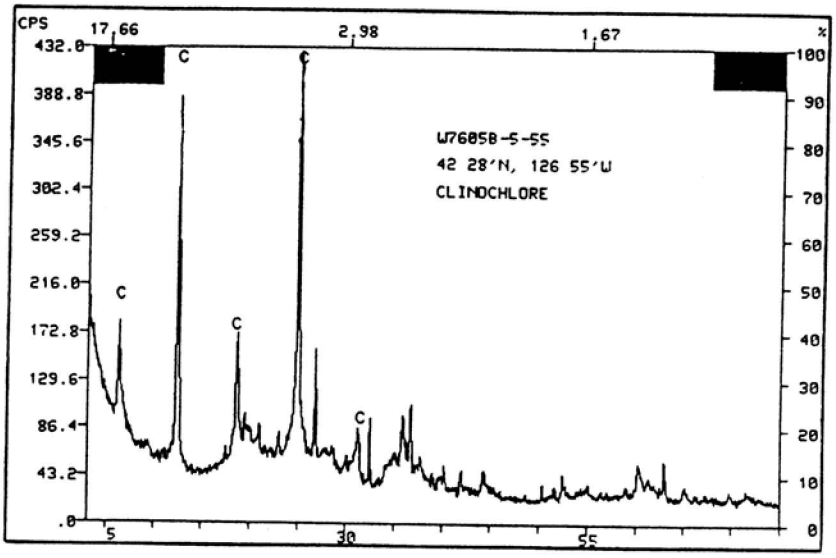

Figure 4: X-ray diffraction spectrum of sample W7605B-5D-55 showing the major peaks for clinochlore (labeled C). Other major peaks are from SiO_2 internal standard.

internal SiO_2, standard, or are unidentified peaks. The X-ray diffractogram of a sample composed predominantly of talc (major peaks labeled T) is shown in Figure 5.

Minerals identified by X-ray diffraction are listed in four Tables: Table 3 for OSU cruise W7605B dredge collection; Table 4 for cruise L5-85-NC ridge axis samples; Table 5 for cruise L5-85-NC off axis samples; and Table 6 for cruise L5-85-NC President Jackson Seamount samples. Mineralogy is based on cumulative analyses of several samples from each dredge site. Most samples display albite peaks in their X-ray spectra and many contain one or more clay minerals. Peaks identified as kaolinite may also represent the presence of amesite, an Al-rich serpentine with a similar diffraction pattern (Haymon and Kastner, 1986b). Clays, including hydrothermal clays such as nontronite and sepiolite, identified by X-ray diffraction will require further analysis to determine the specific minerals present.

Atomic Absorption

Atomic absorption analyses for samples from cruise L5-85-NC are listed in Table 7 for on-axis, off-axis and seamount samples. The highest concentrations of Cu, Ni, Zn, Co, and Ba generally occur in samples high in Mn indicating that these elements are contained in Mn oxide compounds (Toth, 1980). Examination of plots of Fe, Cu, Ni, Zn, Co, and Ba versus Mn (Figures 6 to 11) lead to the following conclusions:

(1) President Jackson Seamount precipitates exhibit higher Fe/Mn and Co/Mn ratios and slightly lower Zn/Mn ratios than Gorda Ridge precipitates (Figs. 6,10 and 9).

(2) Ni and Zn are strongly correlated with Mn (Figs. 8 and 9).

(3) Cu, Co and to a lesser extent Ba versus Mn plots are characterized by two separate trends (Figs. 7a,7b,10 and 11).

DISCUSSION

The results presented above are in agreement with the results of Clague et al (1984) which indicate that hydrothermal activity has been pervasive throughout the study area. Precipitates on OFF AXIS samples are much thicker than those on samples recovered from the ridge axis. This suggests that hydrothermal activity is not necessarily confined to localized vents on the ridge axis, but may also be associated with tectonic features on rift valley walls (Rona, 1986).

Since Fe and Mn oxides are often amorphous, X-ray diffraction results are difficult to compare with results from atomic absorption. However, samples containing large amounts of Mn exhibit corresponding enrichment in Cu, Ni, Co and Zn and their X-ray patterns contain

TABLE 3
Mineralogy of Gorda Ridge Axis Precipitates
(From W7605B)

DREDGE	SAMPLE ID	COLOR	MINERALOGY
3D	3D-2	white	Albite Clays
3D	3D-11	brown	Mn Oxide
3D	3D-13	brown	Mn Oxide
4D	4D-8	brown	Mn Oxide Boehmite
4D	4D-10	red,green,brown	Clay (nontronite*) Todorokite
4D	4D-14	yellow,white,brown	Albite Talc
5D	5D-13	yellow,white	Albite Illite Mn Oxide
5D	5D-31	brown	Mn Oxide
5D	5D-32	orange	Goethite
5D	5D-55	yellow	Clinochlore Albite Mn Oxide

* not positively identified but has major peak present.

TABLE 4
Mineralogy of Gorda Ridge Axis Precipitates
(From L5-85-NC)

DREDGE	SAMPLE ID	COLOR	MINERALOGY
38D	38D-1	grey	Albite Smectite
39D	39D-3	yellow	Albite Talc Chlorite Natrojarosite* Gypsum*
40D	40D-1	grey,tan	Albite Chlorite Boehmite
42D	Very slight hydrothermal alteration		
43D	43D-1	white,tan	Albite Clays* (mostly amorphous)
44D	44D-1	white,tan	Amorphous
45D	45D-1	grey	Albite Clays

* not positively identified but has two major peaks present

TABLE 5
Mineralogy of Gorda Ridge Off-Axis Precipitates
(From L5-85-NC)

DREDGE	SAMPLE ID	COLOR	MINERALOGY
2D	2D	tan,yellow,white	Boehmite Albite Kaolinite Smectite
3D	3D-1	white	Albite Kaolinite Boehmite Clinochlore Illite* Smectite*
3D	3D-2	tan,brown	Amorphous
4D	4D-1A	grey	Albite Clinochore Sepiolite*
4D	4D-1	yellow	Phillipsite Chlorite Kaolinite Sepiolite* Illite
4D	4D-1B	brown	Todorokite Birnessite* Gypsum* Phillipsite
6D	6D-1A	tan	Albite Kaolinite
6D	6D-1	orange,tan	Albite Kaolinite Chlorite Gypsum Pyrite*
7D	7D-1	white	Albite Kaolinite Gypsum* Calcite*

TABLE 5 (con't)

7D	7D-2	yellow,white	Albite* Kaolinite* (mostly amorphous)
7D	7D-3	blue-green	Albite Nontronite* Kaolinite Illite
8D	8D-2	green,brown	Albite Nontronite* Mn Oxide Clinochlore Kaolinite* Illite
10D	10D-1	brown,yellow,tan	Phillipsite* Mn Oxide* (mostly amorphous)
11D	11D-1	yellow,white,brown	Albite Chlorite* Illite* (mostly amorphous)
13D	13D-1	brown,yellow,white	Kaolinite Illite* Pyrite*
13D	13D-2	white,brown	Albite Gypsum* Kaolinite Illite
13D	13D-3	brown,yellow	Pyrite* (mostly amorphous)

* not positively identified but has major peak(s) present.

TABLE 6
Mineralogy of President Jackson Seamount Precipitates
(From L5-85-NC)

DREDGE	SAMPLE ID	COLOR	MINERALOGY
29D	29D	yellow,brown	Quartz Albite Illite Zeolites Heulandite* Natrolite* Clinoptilolite* Clays Nontronite* Sepiolite* Todorokite
29D	29D-1	brown	Quartz Clays Sepiolite* Heulandite Alunite* Todorokite*
33D	33D-1	yellow	Quartz Albite Goethite Zeolite Kaolinite Illite
34D	34D	orange,brown	Quartz (mostly amorphous)
34D	34D-3	red,brown	Quartz Mn Oxide Zeolites Goethite
36D	36D-2	yellow,brown	Quartz Albite Todorokite

* not positively identified but has two major peaks present.

TABLE 7
Atomic Absorption Analyses of Hydrothermal Precipitates
Collected From the Gorda Ridge and President Jackson Seamounts
(From L5-85-NC)

DREDGE	Mn (%)	Fe (%)	Fe/Mn	Cu (ppm)	Ni (ppm)	Zn (ppm)	Co (ppm)	Ba (ppm)
AXIS SAMPLES								
39D-3	0.0800	3.6700	46	120	80	80	--	--
40D-1	0.1370	5.8100	42	55	122	63	48	200
43D-1	0.2390	2.3600	10	57	120	64	--	0
44D-1	0.0600	5.6600	83	132	220	154	--	--
OFF AXIS SAMPLES								
3D-2	4.5600	8.4300	2	216	1170	281	193	1500
4D-1	0.6140	4.8700	81	137	1400	220	--	--
4D-1A	0.5000	6.6900	13	183	510	275	55	300
4D-1B	24.3000	5.8300	0.24	645	5730	2390	344	1800
6D-1	2.5800	13.1000	5	496	927	256	91	800
6D-1A	1.5900	7.7300	5	285	930	192	82	0
7D-1	0.2530	2.4800	10	271	90	184	--	--
8D-1	4.9300	12.7000	3	333	1340	522	196	1010
8D-2	4.8600	6.2800	1	659	1470	406	208	480
10D-1	7.4900	10.6000	1	436	2440	670	234	800
10D-2	13.7000	11.9000	1	428	3480	1090	462	1600
11D-1	1.4200	6.5000	5	310	433	244	54	400
13D-1	0.8240	7.5600	9	157	158	218	82	820
13D-2	0.0643	2.6400	41	192	137	200	103	10
13D-3	1.8200	5.9500	3	477	460	277	--	0
SEAMOUNT SAMPLES								
29D	3.7400	14.0000	4	229	851	234	702	700
29D-1	1.9700	19.1000	10	250	573	141	499	200
29D-2	3.4600	20.1000	6	286	918	286	611	400
32D-1	10.0000	22.2000	2	183	1910	505	1810	1100
33D-1	2.1000	18.3000	9	623	900	159	450	0
34D	8.1900	17.9000	2	3270	2430	291	2380	500
34D-3	4.9000	19.5000	4	795	2290	435	408	1300
35D-1	0.3970	8.1000	20	124	235	158	118	1000
36D-1A	4.6100	12.7000	3	164	1050	323	665	900
36D-2	3.6400	9.8300	3	333	1160	279	--	1300

(Analyses performed by J. Robbins)

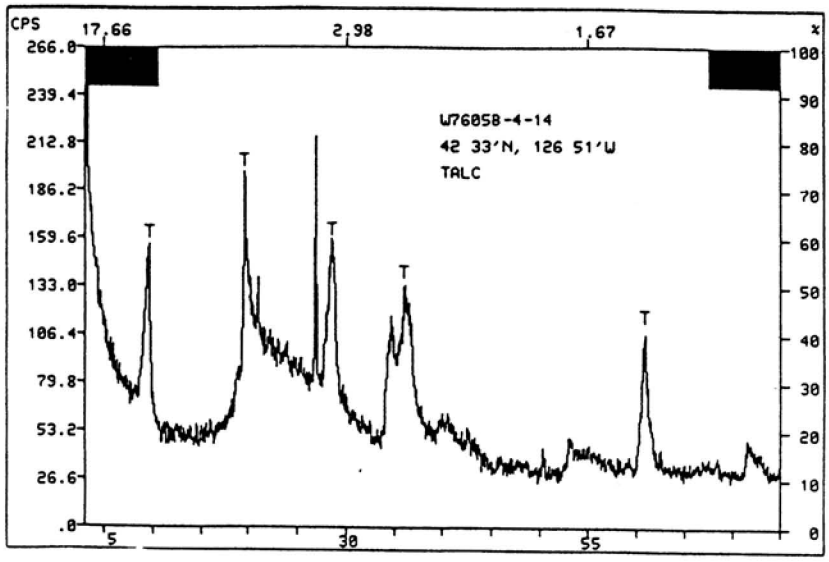

Figure 5: X-ray diffraction spectrum of sample W7605B-4D-14 showing the major peaks for talc. Other peaks present belong to albite and the SiO_2 internal standard.

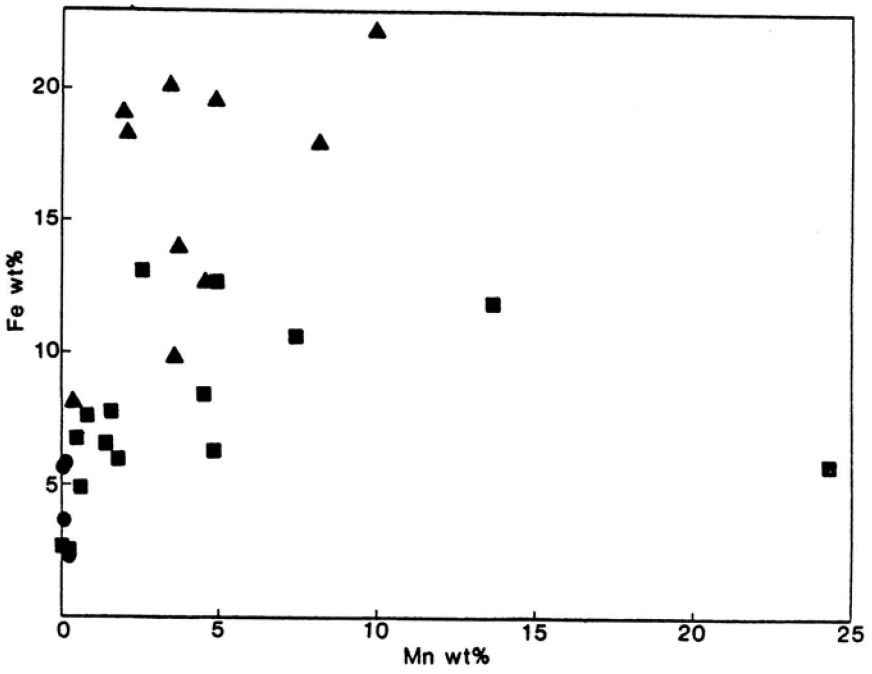

Figure 6: Fe wt% versus Mn wt%. Circles are ON AXIS samples, squares are OFF AXIS samples and triangles are SEAMOUNT samples.

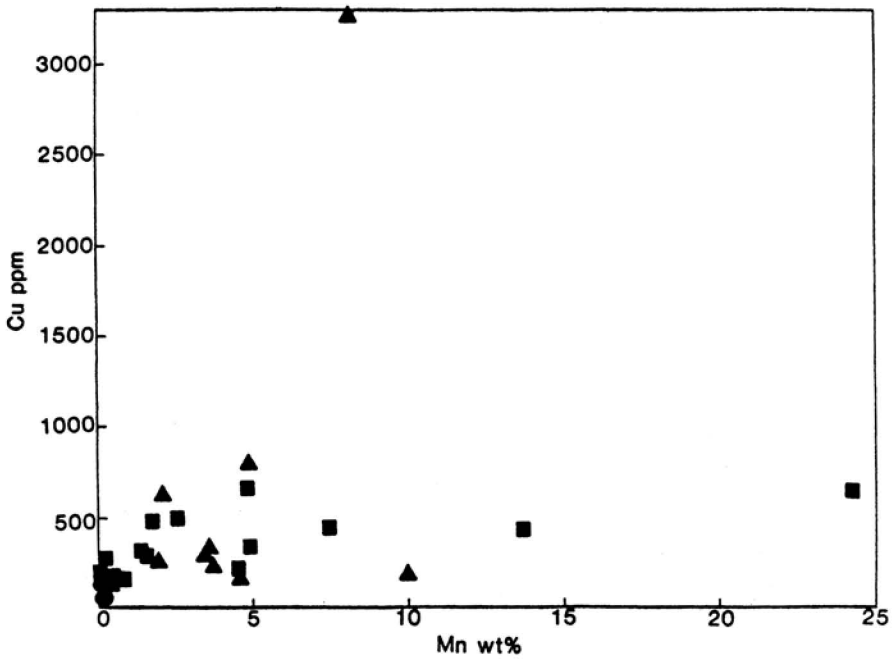

Figure 7a: Cu ppm versus Mn wt%. Symbols are the same as in Figure 6.

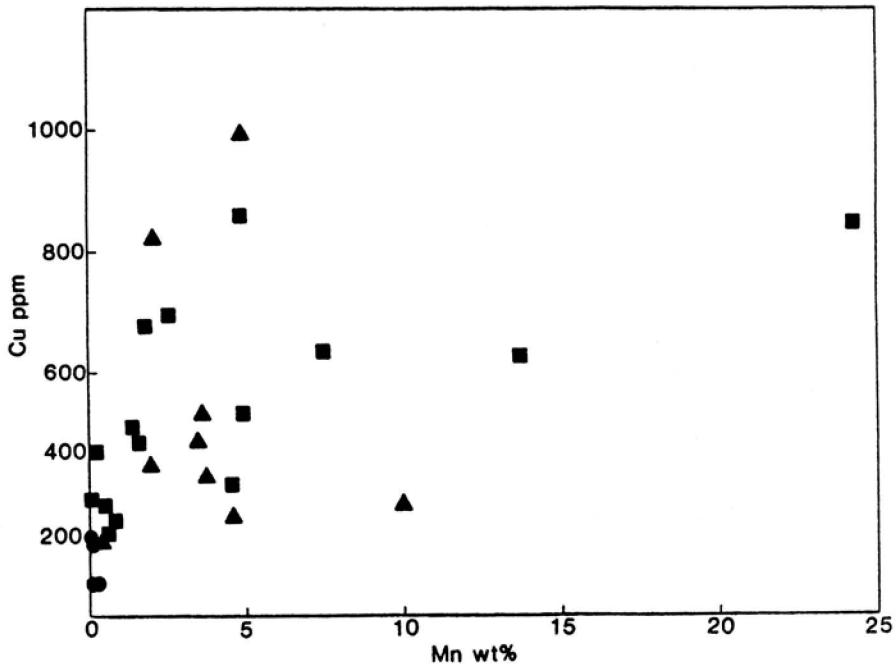

Figure 7b: Cu ppm versus Mn wt%. Same as Figure 7a, but with different scale excluding sample L5-85-NC-34D to show separation of two Cu/Mn trends.

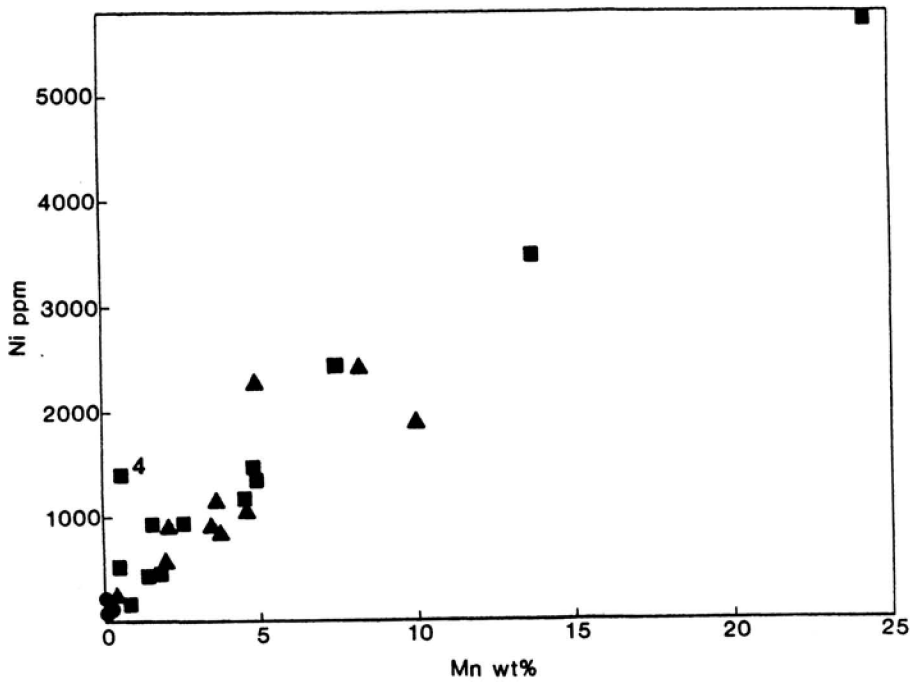

Figure 8: Ni ppm versus Mn wt%. Symbols are the same as in Figure 6. The square labeled 4 is sample L5-85-NC-4D-1 which has a significantly higher Ni/Mn ratio.

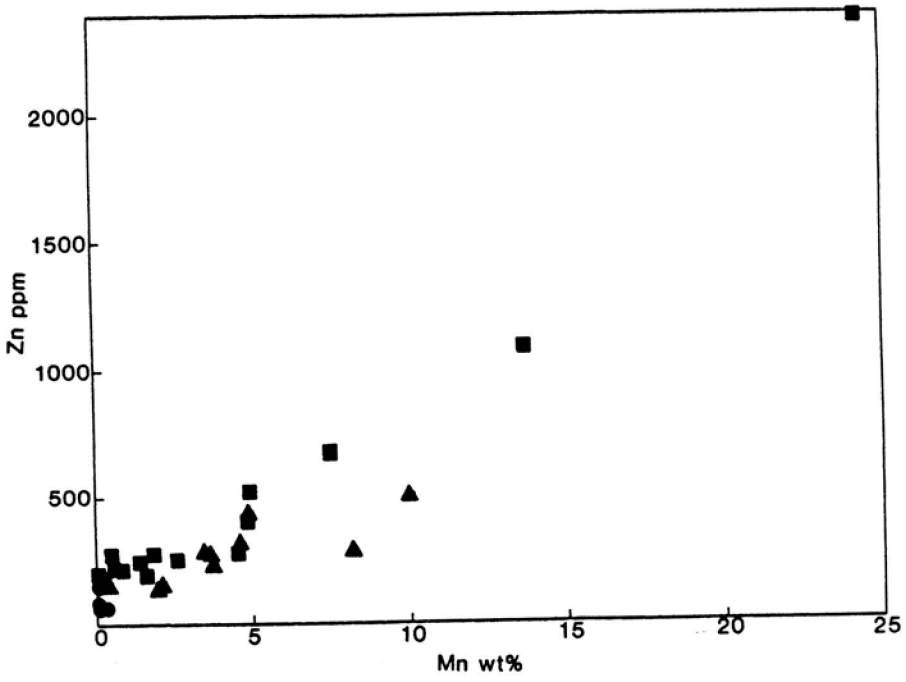

Figure 9: Zn ppm versus Mn wt%. Symbols are the same as in Figure 6.

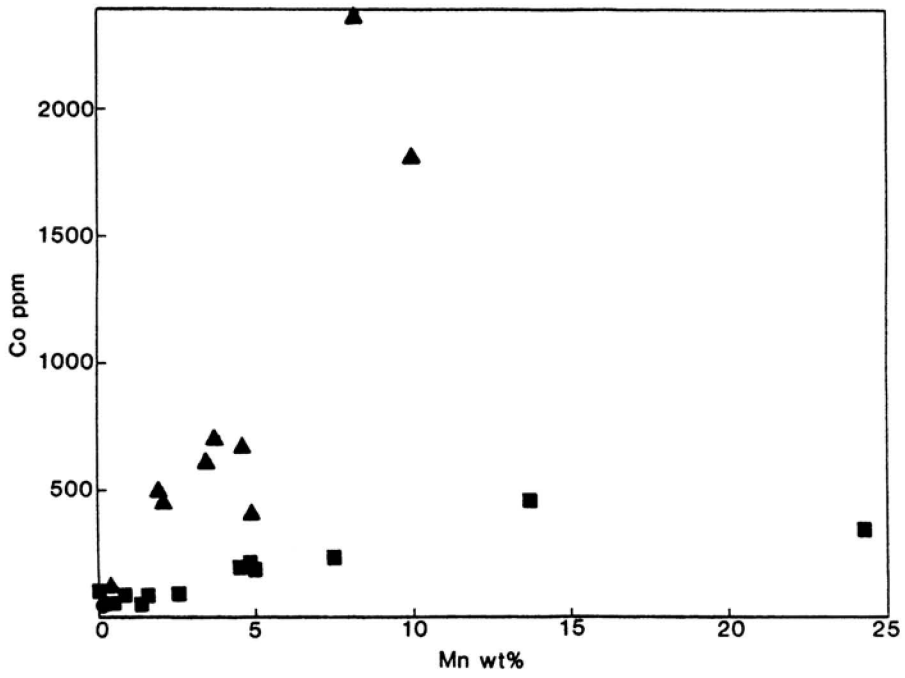

Figure 10: Co ppm versus Mn wt%. Symbols are the same as in Figure 6.

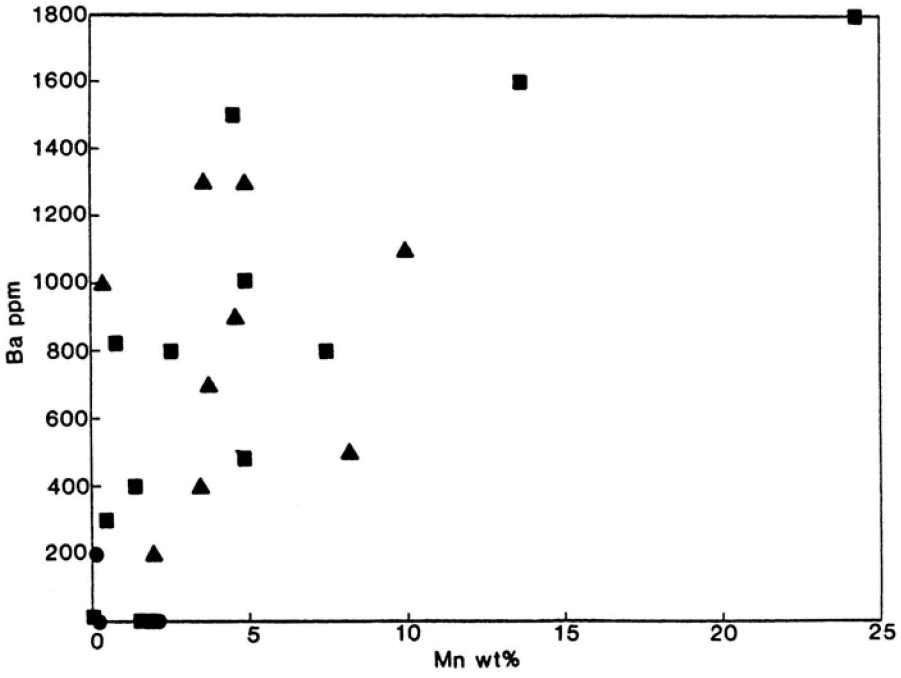

Figure 11: Ba ppm versus Mn wt%. Symbols are the same as in Figure 6.

peaks for Mn oxides. Several of the mineral precipitates identified in this study require restricted thermal and chemical environments for their genesis. Temporal changes in fluid chemistry may result in the formation of a sequence of clay minerals. Mg-rich smectites are expected to precipitate under high water/rock ratios from Mg-rich solutions (Scheidegger and Stakes, 1978). Experimental data indicate that nontronite (an Fe-rich smectite) is formed from solutions relatively low in silica and rich in reduced iron (Fe^{2+}) (Harder, 1976). Smectite forms under alkaline conditions, but kaolinite and boehmite which coexist in several samples imply extremely acid conditions (Deer et al., 1966). In many dredges, there is an indication that several clay minerals occur together and further analysis may help to explain the chemical evolution of the hydrothermal fluids.

Evidence of iron oxides and hydrated iron oxides found in many samples suggests the occurrence of low temperature alteration of sulfides in an oxidizing environment (Hekinian et al, 1980). Secondary pyrrhotite still preserved and identified in hand sample (Ship's Records on L5-85-NC-3D) indicates that the fs_2 and fo_2 is relatively low and temperature of deposition is between 320-380°C (Haymon and Kastner, 1986b, Koski et al, 1985). Pyrite (tentatively identified in L5-85-NC-6D and L5-85-NC-13D) requires slightly higher fs_2 than pyrrhotite (Koski et al., 1985). The presence of talc (W7605B-4D-14and L5-85-NC-39D) indicates that temperatures of deposition were probably in the range of 270-500°C and that the fluid from which it precipitated was relatively silica-rich (Mottl, 1983, Koski et al, 1985). Smectites identified in many samples could indicate temperatures of deposition as high as 295-360°C if they are determined to be similar to smectites collected from the East Pacific Rise (Haymon and Kastner, 1986b).

In sample W7605B-5D-55, the presence of both albite and clinochlore indicates a temperature of deposition of about 300°C. If both minerals precipitated together in equilibrium, then the fluid was characterized by low Fe concentration and Mg concentration restricted to a very narrow range (Koski et al, 1985). However, mass transfer calculations indicate that albite and clinochlore form under different water/rock ratios which suggests changing conditions between deposition of the two minerals, with albite preserved under conditions incompatible with its formation (Gitlin, 1985).

The general lack of correlation between Fe and Mn confirms that Fe is incorporated in other mineral phases in addition to Mn oxides. The high Fe/Mn ratios of many samples (Table 7, Figure 6) probably results from extreme fractionation of Fe and Mn typical of hydrothermal areas where Fe precipitates more rapidly as Fe-rich sulfides, clays and Fe oxides and hydroxides before Mn precipitates (Corliss et al., 1978, Lyle, 1981). Assuming the composition of hydrothermal fluids was similar at both localities, a more active hydrothermal system may have increased Fe/Mn ratios in seamount

precipitates relative to Gorda Ridge precipitates. (Hekinian and Fouquet, 1985). In addition, lower exit temperatures of hydrothermal fluids may have caused slightly lower Zn/Mn ratios in seamount samples if higher temperature Zn sulfides precipitated at depth (Hekinian and Fouquet, 1985). Alternatively, because seamount peaks are sites of intensified currents (Genin et al., 1986), differential weathering may have lowered the Zn/Mn ratio and raised the Co/Mn ratio in seamount samples. However, many authors contend that the oxidizing environment at seamounts oxidizes Co^{2+} to Co^{3+} which substitutes for Mn^{4+} in greater quantity in Mn oxide phases (Burns, 1976, Chave et al., 1986). Volcanic activity at the seamounts may have provided an enriched source of cobalt (Frazer and Fisk, 1981).

The higher Cu/Mn ratios of some samples cannot be attributed to a change in oxidation state, however, since Cu oxidation states are either +1 or +2 and only the +2 state subsitutes into Mn oxide phases. Hence, the higher Cu/Mn ratios of some samples requires that (1) there is a greater source of Cu at these sites which may be incorporated in sulfides or sulfates, (2) different Mn oxide phases which can uptake greater amounts of Cu are present in these samples, or (3) Cu is the favored cation in Mn oxides since other cations are proportionally lower at these sites. The third possibility can be ruled out since Table 6 shows no corresponding depletion in other trace metals with Cu enrichment. The second possibility is difficult to resolve since some Mn oxides may be amorphous in several samples. Also, little is known about the relative capacities of trace metal uptake in different Mn minerals (Chave et al, 1986). Since hydrothermal areas have been noted for their great elemental variations (Edmond et al., 1979), the first possibility suggested above seems the most reasonable. Variations in source composition may also explain secondary trends noted for Co/Mn and Ba/Mn (Figs. 10 and 11) and the high Ni/Mn ratio exhibited by sample 4D-1 (Fig. 6).

Samples with high Fe/Mn ratios are believed to be close to the hydrothermal vent sites because of the extreme fractionation of Fe and Mn. Also, samples with high Cu, Ni, Co, Zn, or Ba/Mn ratios indicate that these elements are contained in other mineral phases besides Mn oxides, such as sulfides and sulfates (clays and Fe oxides uptake far less of these elements than Mn oxides). Thus samples with both high Fe/Mn ratios and high trace metal contents relative to Mn may be close to hydrothermal vent sites. Figure 12 presents the abundance of trace metals with respect to Fe and Mn in a ternary diagram after Bonatti et al, 1972. Several samples plot in the hydrothermal field of Bonatti et al, 1972 and many samples plot in fields (labeled hydrogenous and Fe-Mn crusts) which may be interpreted as deposits enriched with trace metals by seawater (Toth, 1980). However, two samples with very high Fe/Mn ratios (4D-1 and 13D-2) also have high Cu+Ni+Co relative to Fe and Mn. These samples may have anomalous enrichment in trace metals without concurrent enrichment in Mn because these elements are contained in sulfides or sulphates implying high temperature hydrothermal venting . These two

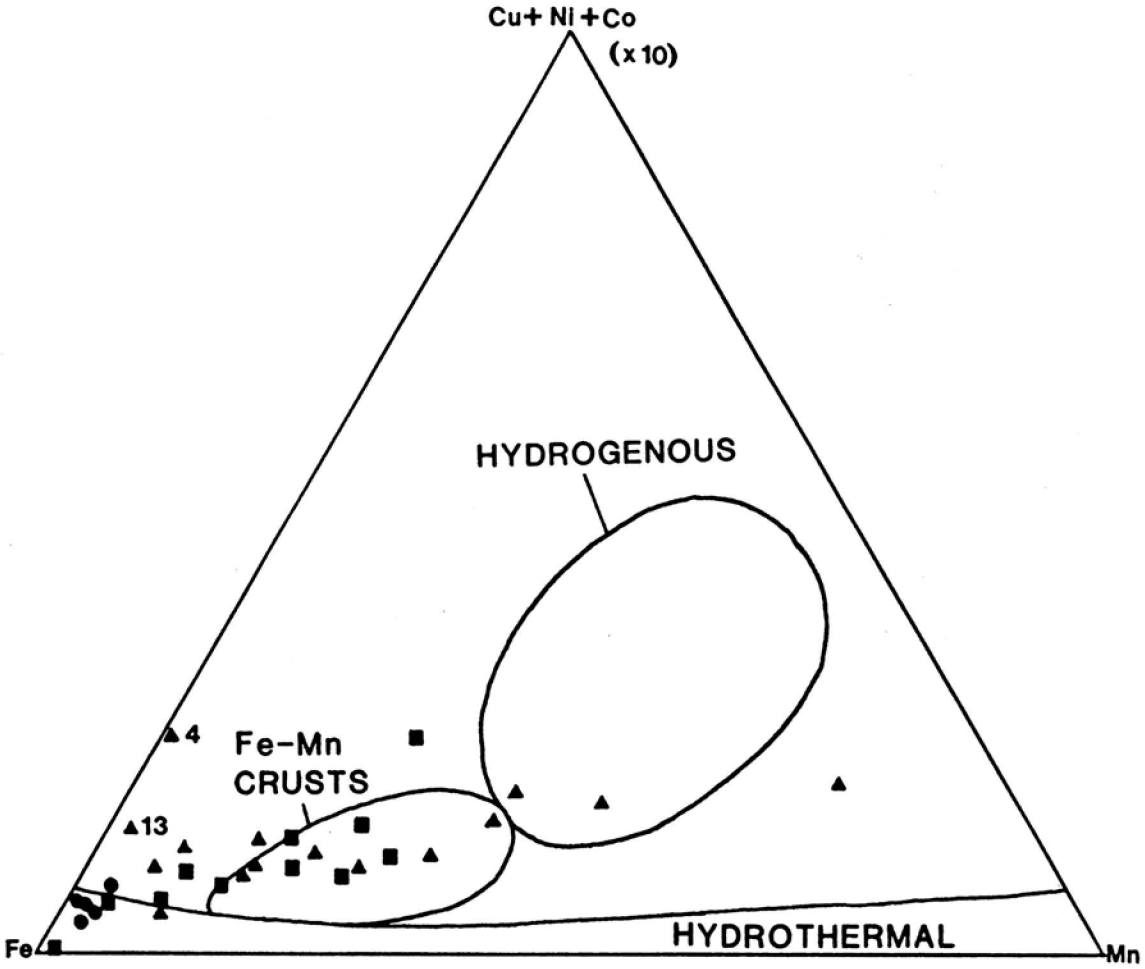

Figure 12: Ternary plot with apices Fe, Mn, and Cu+Ni+Co(x10) after Bonatti et al., 1972. Squares are off axis samples, triangles are seamount samples and circles are on axis samples. Samples designated 4 and 13 are L5-85-NC-4D-1 and L5-85-NC-13D-2 respectively. Hydrothermal, hydrogenous and Fe-Mn crust fields are from Toth, 1981.

locations, along with other regions with high Fe/Mn ratios along the ridge axis (Table 7) appear to be the best prospects for hydrothermal vent sites, based on the samples in this study.

FUTURE WORK

To test this method of prospecting for hydrothermal vents, future diving and dredging operations should be directed in the vicinity of sites with high Fe/Mn ratios and high trace metal/Mn ratios determined in this study. As previously mentioned, these are L5-85-NC-4D and L5-85-NC-13D. More recent 1986 cruises recovered hydrothermal precipitates from the northern Gorda Ridge axial valley and deposits from the Escanaba sedimented hydrothermal system in the southern Gorda Ridge segment. The samples from the northern Gorda Ridge were collected in the vicinity of previously recovered precipitates with high Fe/Mn ratios. Further analytical work on these recently recovered samples should help to determine if regional geochemical patterns exist in the hydrothermal precipitates and if significant differences can be established between the hydrothermal systems of the northern and southern segments of the Gorda Ridge. XRD and atomic absorption will be used to determine mineralogy and concentration of valuable metals. Additional analyses by electron microprobe and SEM/EDS will be useful to determine the chemistry of individual mineral species and mineral morphology which may enhance our understanding of mechanisms of hydrothermal mineral growth. Temperatures of deposition of clay minerals can be determined by oxygen isotope analysis and these may be incorporated with AA data to assist in locating hydrothermal vent sites.

It may be necessary to separate some of the clay minerals and other silicates from the heavy minerals by centrifuge, by heavy liquids (eg. sodium metatungstate to separate sulfides), or by chemical techniques (eg. to remove oxides and separate sulfates) for XRD analysis to determine if sulfides, sulfates and exotic minerals such as arsenates, selenides, borates or phosphates are present. This process could be performed on 1986 cruise samples which have enough material available.

CONCLUSIONS

The mineral encrustations that we collected from the surfaces of many basalts from the northern end of the Gorda Ridge are definitely of hydrothermal origin. Minerals present in some of these encrustations such as talc and pyrrhotite, indicate that they were deposited at high temperatures. These samples were collected from both the axial valley and the valley walls, therefore, each of these regions is or was recently hydrothermally active. It is possible that locating hydrothermal precipitates with high Fe/Mn and trace metal/Mn ratios may prove useful as a prospecting tool for locating hydrothermal vents. Two geochemically anomalous regions have been targeted for further investigations to test this hypothesis. Our results indicate

that hydrothermal vents and associated polymetallic sulfide deposits are likely to exist in the area of the northern Gorda Ridge near its intersection with the Blanco Fracture Zone.

ACKNOWLEDGEMENTS

We wish to thank the chief scientists of the S.P. Lee (David Clague, Randy Koski, and Andy Stevenson) as well as captain, crew and scientific party of L5-85-NC for their help and hospitality. Greg Campi helped us continually with the x-ray diffraction operation and analyses and Jim Robbins analyzed the deposits by AA. Helpful discussions and assistance were provided by Mitch Lyle, Curt Peterson, Roger Hart and Doug Pyle. This manuscript was greatly improved by the reviews of Joe Ritchey and Dave Clague.

REFERENCES

Bäcker, H., J. Lange, and V. Marchig. 1985. Hydrothermal activity and sulfide formation in axial valleys of the East Pacific Rise crest between 18 and 22°S. Earth Planet. Sci. Lett. 72:9-22.

Bonatti, E., T. Kraemer and H. Rudell. 1972. Classification and genesis of submarine iron-manganese deposits, p.149-166. In D.R. Horn (ed.), Papers on a Conference about Ferromanganese Deposits on the Ocean Floor. Washington, D.C., National Sciene Foundation.

Burns, R.G. 1976. The uptake of cobalt into ferromanganese nodules, soils and synthetic manganese (IV) oxides. Geochim Cosmochim Acta. 40:95-102.

Chave, K.E., C.L. Morgen, and W.J. Green. 1986. A geochemical comparison of manganese oxide deposits of the Hawaiian Archipelago and the Deep Sea. Applied Geochem. 1:223-240.

Clague, D.A., W. Friesen, P. Quinterno, M. Holmes, J. Morton, R. Bouse, L. Morgenson, and A. Davis. 1984. Preliminary geological, geophysical and biological data from the Gorda Ridge, U.S. Geol. Survey Open-File Report 84-364, 48p.

Corliss, J.B., M. Lyle, J. Dymond, and K. Crane. 1978. The chemistry of hydrothermal mounds near the Galapagos Rift. Earth Planet. Sci. Lett. 40:12-24.

Deer, W.A., R.A. Howie and J. Zussman. 1966. An introduction to the rock forming minerals. Longman Group Limited, London.

Dymond, J. 1981. Geochemistry of Narca plate surface sediments: an evaluation of hydrothermal, biogenic, detrital and hydrogenous sources. Geol. Soc. Am. Mem. 154:133-173.

Edmond, J.M., C. Measures, B. Mangum, B. Grant, F.R. Sclater, R. Collier, A. Hudson, L.I. Gordon and J.B. Corliss. 1979. On the formation of metal-rich deposits at ridge crests. Earth Planet. Sci. Lett. 49:19-30.

Frazer, J.Z. and M.B. Fisk. 1981. Geological factors related to characteristics of sea-floor manganese nodule deposits. Deep-Sea Res. 28A:1533-1551.

Genin, A., P.K. Dayton, P.F. Lonsdale and F.N. Spiess. 1986. Corals on seamount peaks provide evidence of current acceleration over deep-sea topography. Nature. 322:59-61.

Gitlin, E. 1985. Sulfide remobilization during low temperature alteration of seafloor basalt. Geochim. Cosmochim. Acta. 49: 1567-1579.

Harder, H. 1976. Nontronite synthesis at low temperatures. Chem. Geol. 18:169-180.

Haymon, R.M. and M. Kastner. 1981. Hot spring deposits on the East Pacific Rise at 21°N: preliminary description of mineralogy and genesis. Earth Planet. Sci. Lett. 53:363-386.

Haymon, R.M. and M. Kastner. 1986a. Caminite: A new magnesium-hydroxide-sulfate-hydrate mineral found in a submarine hydrothermal deposit, East Pacific Rise, 21°N. Am. Min. 71: 819-825.

Haymon, R.M. and M. Kastner. 1986b. The formation of high temperature clay minerals from basalt alteration during hydrothermal discharge on the East Pacific Rise axis at 21°N. Geochim. Cosmochim. Acta. 50:1933-1939.

Hekinian, R., M. Fevrier, J.L. Bischoff, P. Picot and W.C. Shanks 1980. Sulfide deposits from the East Pacific Rise near 21°N. Science. 207:1433-1444.

Hekinian, R., V. Renard and J.L. Cheminee. 1983. Hydrothermal deposits on the East Pacific Rise near 13°N: Geological setting and distribution of active sulfide chimneys, p.571-594. In P.A. Rona, K. Bostrom, L. Laubier and K.L. Smith, Jr. (eds.), Hydrothermal Processes at Seafloor Spreading Centers. Plenum Press, New York.

Hekinian, R. and Y. Fouquet. 1985. Volcanism and metallogenesis of axial and off-axial structures on the East Pacific Rise near 13°N. Econ Geol. 80:221-249.

Humphries, S. and G. Thompson. 1978. Trace element mobility during hydrothermal alteration of oceanic basalts. Geochim Cosmochim Acta. 42:127-136.

Koski, R.A., D.A. Clague and E. Oudin. 1984. Mineralogy and chemistry of massive sulfide deposits from the Juan de Fuca Ridge. Geol. Soc. Am. Bull. 95:930-945.

Koski, R.A., P.F. Lonsdale, W.C. Shanks, M.E. Berndt and E.E. Howe. 1985. Mineralogy and geochemistry of a sediment-hosted

hydrothermal sulfide deposit from the southern trough of Guaymas Basin, Gulf of California. J. Geophys. Res. 90:6695-6707.

Lafitte, M., R. Maury, E.A. Perseil and J. Boulegue. 1985. Morphological and analytical study of hydrothermal sulfides from 21° north East Pacific Rise. Earth Planet. Sci. Lett. 73: 53-64.

Lyle, M., 1981. Formation and growth of ferromanganese oxides on the Nazca plate. Geol. Soc. Am. Mem. 154:269-293.

Mottl, M.J., 1983. Hydrothermal processes at seafloor spreading centers: application of basalt-seawater experimental results, p.199-224. In P.A. Rona, K. Bostrom, L. Laubier and K.L. Smith, Jr. (eds.), Hydrothermal Processes at Seafloor Spreading Centers. Plenum Press, New York.

Oudin, E., 1983. Hydrothermal sulfide deposits of the East Pacific Rise (21°N) Part I: Desciptive mineralogy. Mar. Mining. 4: 39-72.

Rona, P.A., G. Klinkhammer, T.A. Nelson, J.H. Trefry and H. Elderfield. 1986. Black smokers, massive sulfides and vent biota at the Mid-Atlantic Ridge. Nature. 321:33-37.

Roth, S. and J. Dymond, 1985. Hydrothermal particle flux: Endeavour Ridge phase I. EOS. 66:930.

Scheidegger, K.F. and D.S. Stakes. 1978. X-ray diffraction and chemical study of secondary minerals from DSDP Leg 51, Sites 417A and 417D. p.1253-1263. In T. Donnelly, J. Francheteau, W. Bryan, P. Robinson, M. Flower, M. Salisbury, et al., Initial Reports of the Deep Sea Drilling Project, v. 51,52,53 Part 2: Washington (U.S. Government Printing Office).

Seyfried, W.E. and J.L. Bischoff. 1979. Low temperature basalt alteration by seawater: An experimental study at 70°C and 150°C. Geochim. Cosmochim. Acta. 43:1937-1947.

Singer, A. and P. Stoffers. 1981. Hydrothermal vermiculite from the Atlantis II Deep, Red Sea. Clays and Clay Minerals. 29:454-458.

Thompson, G. 1983. Basalt-seawater interaction, p225-278. In P.A. Rona, K. Bostrom, L. Laubier and K.L. Smith, Jr. (eds.), Hydrothermal Processes at Seafloor Spreading Centers.

Thompson, G., M.J. Mottl and P.A. Rona. 1985. Morphology, mineralogy and chemistry of hydrothermal deposits from the TAG area, 26°N Mid Atlantic Ridge. Chem. Geol. 49:243-257.

Toth, J.R. 1980. Deposition of submarine crusts rich in manganese and iron. Geol. Soc. Am. Bull. 91:44-54.

von Damm, K.L., J.M. Edmond, C.I. Measures, and B. Grant. 1985 Chemistry of submarine hydrothermal solutions at Guaymas Basin, Gulf of California. Geochim. Cosmochim. Acta 49:2221-2237.

Whitney, G. 1983. Hydrothermal reactivity of saponite. Clays and Clay Minerals. 31:1-8.

Wilde, P., T.E. Chase, M.L. Holmes, W.R. Normark, J.A. Tomas, D.S. McCulloch and L.D. Kulm. 1978. Oceanographic data off northern California-southern Oregon, 40° to 43° North including the Gorda Deep Sea Fan. LBL Publ. 251, Lawrence Berkeley Lab. Berkeley, Calif.

Wilde, P., T.E. Chase, M.L. Holmes, W.R. Normark, J.A. Tomas, D.S. McCulloch, P.R. Carlson, L.D. Kulm and J.D. Young. 1979. Oceanographic data off Oregon 43° to 46° North including Astoria Deep-Sea Fan. LBL Publ. 253, Lawrence Berkeley Lab, Berkeley, Calif.

Wirsching, U. 1981. Experiments on the formation of calcium zeolites. Clays and Clay Minerals. 29:171-183.